Quantifying the impact of small variations in fracture geometric characteristics on peak rock mass properties at a mining project using a coupled DFN–DEM approach

Martin Grenon, Genevieve Bruneau, and Iris Kapinga Kalala

Faculté des sciences et de génie, Département de génie des mines, de la métallurgie et des matériaux, Université Laval, Québec, Canada

ABSTRACT
Using field data from Agnico-Eagle's Meliadine gold project located in Nunavut Territory in northern Canada, a coupled DFN–DEM approach was used to evaluate the rock mass mechanical properties at REV. Variability in the structural data gathered on site and the variability associated with the stochastic modeling process have an impact on discrete fracture model (DFN) properties. Through a sensitivity analysis, this paper assesses the influence of a variation in the DFN model input parameters' values on the rock mass peak properties – uniaxial compressive strength, Young modulus and Poisson ratio. The results not only highlight the possibilities associated with DFN–DEM modeling in characterizing rock mass properties at the engineering scale, they also provide a systematic way to assess the critical structural parameters controlling the rock mass properties.

KEYWORDS
Rock mass properties, Discrete Fracture Network (DFN), Distinct Element Method (DEM), Coupled DFN–DEM approach, Sensitivity analysis

CITATION
Grenon M, Bruneau G, & Kalala I. K. Quantifying the impact of small variations in fracture geometric characteristics on peak rock mass properties at a mining project using a coupled DFN–DEM approach. Computers and Geotechnics (2014) 58, 47-55.

This is the author's version of the original manuscript. The final publication is available at Elsevier Link Online via http://dx.doi.org/10.1016/j.compgeo.2014.01.010

1 INTRODUCTION

Determining the properties of rock masses at the scale of an engineering work is an essential part of the engineering design process. In practice, this is commonly achieved by using an empirical approach such as the Hoek–Brown failure criterion, Hoek [1], Cai et al. [2], Alejano et al. [3]. Alternatively, recent work showed the potential of numerical modeling approaches combining Discrete Fracture Network (DFN) modeling and Distinct Element Mod eling (DEM) to derive rock mass properties at engineering problem scale, Mas Ivars et al. [4], Esmaieli et al. [5], Harthong et al. [6]. Although the DFN–DEM approach is not routinely used at the current time, due mainly to computing time limitation, it is clearly a potentially interesting way to better understand the behavior of fractured rock masses.

DFN modeling relies heavily on the quality of structural data on natural fractures gathered in the field. The principal geometric properties of a fractured rock mass (orientation, size and frequency) are obtained through two sampling strategies: borehole sampling and examination of an exposed rock face, [7]. Uncertainties are associated with the sampled data. Fracture data uncertainty stems from the recurrent difficulties geologists, engineering geologists and geotechnical engineers face in

correctly predicting the inherently variable properties and characteristics of a fractured rock mass, [8].

Furthermore, variability in modeled DFN properties is observed due to the stochastic nature of the fracture generation process. The same input parameters will result in a range of possible DFNs which are all possible representations of the structural field conditions.

Referring to a mining case study located in the Canadian Arctic, this paper addresses the impact of varying DFN input parameters' values – from a base case scenario – on the rock mass mechanical properties (Uniaxial Compressive Strength (UCS), Young's Modulus (E) and Poisson ratio (ν)) using DFN–DEM modeling. The work was performed using the methodology proposed by Esmaieli et al. [5] to assess peak rock mass properties using DFN–DEM modeling. This paper also describes the possibilities as well as the limitations of this modeling approach at this point in time.

2 CASE STUDY

The Meliadine gold mine project in Nunavut Territory in northern Canada (Fig. 1) is Agnico-Eagle's second major project in Canada's Low Arctic, the Meadowbank gold mine being the first. As of December 31, 2010, the project has probable gold reserves of 2.6 million ounces (9.5 million tons grading 8.5 g/ton gold). Meliadine is located on a large property with significant exploration upside and has regional synergies with Meadowbank, located just 290 km to the northwest.

A significant portion of the Tiriganiaq gold deposit, on the Meliadine property, will be mined through an open pit operation. The projected ultimate pit, obtained at the feasibility study, was 1050 m x 390 m in surface area, and extended to a depth of 155 m. The mechanical and structural properties were obtained through line mapping, oriented drilling, and laboratory testing. The entire pit area was defined by a single structural domain. Four fracture sets were identified, with the most dominant one being the foliation, and the second most dominant set being J0. Fracture orientations were defined by their mean dip and dip direction and a Fisher coefficient, while the mean trace length values were obtained through face mapping in underground access drifts.

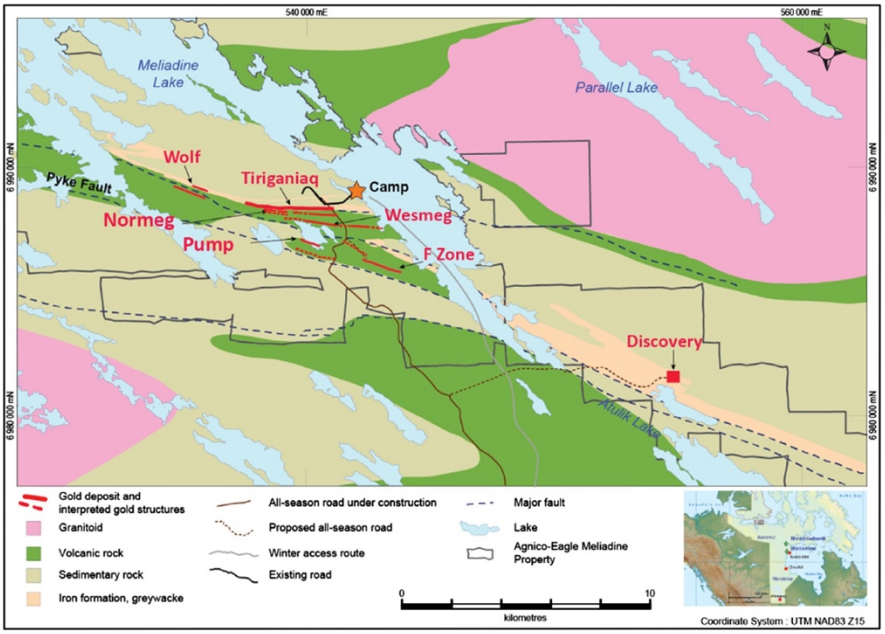

Fig. 1. Meliadine gold mine project location map, [9].

3 MODELING WORKFLOW

The workflow used in building a numerical rock mass model consists of three principal components: a DFN, a DEM model and a combined DFN–DEM model. These steps are schematized in Fig. 2. This is commonly performed at various sample sizes to arrive at a Representative Elemental Volume (REV) for rock mass properties.

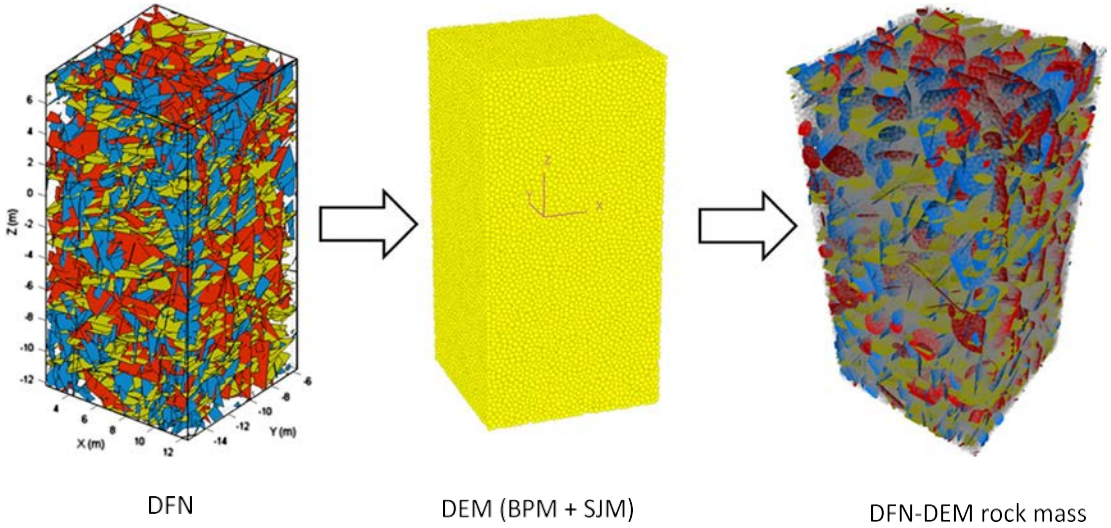

Fig. 2. DFN–DEM rock mass modeling workflow – where DFN means Discrete Fracture Network, DEM corresponds to Distinct Element Model, BPM stands for Bond Particle Model and SJM for Smooth Joint Model.

3.1 DFN

The first step of the workflow is to model a DFN. A DFN model is a stochastic model that represents the rock mass joint fabric. The fundamentals of stochastic modeling are discussed in detail by Dershowitz and Einstein [10], where they demonstrate that DFN models can be used to represent rock mass fracture geometry as an entity.

The Fracture-SG code, Grenon [11], was used for generating the DFN model for the Meliadine mining project. It is based on a modified Veneziano model, which assumes that fractures are polygons. The fracture network generation starts with a primary process consisting of a Poisson network of planes in 3D space followed by a secondary process of tessellation with a Poisson line process that makes polygonal shape fractures. During the secondary process, all fractures on a given generation planes are coplanar. Field observations may indicate that this is not a valid assumption. A third process aiming at overcoming this limitation of the Veneziano model was introduced. This process consists of a simple translation rule based on fracture size implemented within Fracture-SG, Grenon and Hadjigeorgiou [12], following the recommendations of Meyer [13].

Fracture properties (orientation, spacing and trace length) were obtained at the mining site using various field techniques (oriented core sampling, line mapping and window mapping). Within Fracture-SG, the input parameters used to generate the DFN are fracture sets mean orientation (dip and dip direction), fracture sets orientation dispersion (Fisher coefficient – K), fracture volumetric intensity (P32 – total fracture area per volume, [14]) and fracture area ($\bar{A}$). The DFN was calibrated comparing the modeled data with field observations. The forward modeling approach was used to match DFN model properties with field data. Several DFN models were used to arrive at a satisfactory statistical agreement between model and in situ conditions. Several authors are using this calibration method, Grenon and Hadjigeorgiou [15], Dershowitz [16] and others. For the

Meliadine case study, the detailed calibration procedure is presented in Kapinga Kalala [17]. The calibrated DFN has 112,032 fractures and is 50 m x 50 m x 50 m in size. The calibrated model's input parameters are presented in Table 1.

Table 1. Input parameters for the calibrated DFN model

	Dip (°)	Dip direction (°)	K	P32 (m^2/m^3)	Area (m^2)
Foliation	67	003	172	10.8	15
J0	24	184	64	3.8	51
J1/J3	75	100	36	4.5	12
J2	36	271	17	1.3	15

3.2 DEM

The second step of the workflow is to calibrate intact and fracture properties within a DEM model. The distinct element modeling (DEM) Particle Flow Code (PFC3D) developed by Itasca was used in this project. Within the DEM, the intact rock is simulated as an assembly of rigid spherical particles bonded together at their contact points. The physical behavior of contacts is described either by a Bond Particle Model (BPM) – linear contact – or a Smooth Joint Model (SJM) – frictional sliding model.

The BPM properties are meant to enable the DEM to replicate the intact rock behavior, and the SJM properties aim to allow the DEM to reflect the behavior of a joint – if the contact between particles corresponds to a fracture.

3.2.1 Calibrating intact rock properties

A procedure to generate and calibrate a bonded particle model (BPM) for intact rock simulation was proposed by Potyondy and Cundall [18]. A bonded particle model portrays an intact rock as packed non-uniform spherical particles that are connected together at their contact points with parallel bonds. An inverse calibration method is used to establish the micro-mechanical input parameters for the BPM that result in appropriate intact rock properties obtained from laboratory tests on rock samples. The approach was used by several authors, Mas Ivars et al. [4], and Esmaieli et al. [5].

For this project, the micro-properties were calibrated to match a UCS value of 80% of the average laboratory uniaxial compressive strength obtained on 50-mm diameter core samples. This ratio was selected after the guidelines proposed by Hoek [1], Yoshinaka [19] and Cai et al. [20]. The calibration, therefore, targeted a UCS of 92 MPa, a Young modulus of 55 GPa and a Poisson ratio of 0.3. A minimum particle radius of 0.05 m was used for the intact rock simulation in the BPM. This size is roughly one-fifth of the fracture spacing as suggested by Mas Ivars [4]. The detailed BPM calibration process for the Meliadine case study is presented in Kapinga Kalala [17].

3.2.2 Calibrating fracture properties

A BPM can represent a homogeneous rock, or it can be divided into a number of blocks by fractures. The properties of particles and bonds along the fracture planes are usually different from those that exist in the intact parts of the model. The Smooth Joint Model (SJM) was used to simulate the mechanical behavior of fractures. This model ensures sliding of rock blocks along the fracture planes, Mas Ivars et al. [21]. Using the calibrated DEM for intact rock, a triaxial test was numerically

conducted on four specimens, each intersected by a fracture at different inclinations. The testing procedure employed has been described in detail elsewhere, Esmaieli et al. [5]. The model was calibrated to assign the necessary micro-mechanical properties to the particles along the fracture planes to match laboratory results for shear tests performed on natural discontinuities by Golder [22]. These tests suggested that the foliation has a friction angle of 34° and cohesion of 0 kPa. The other three fracture sets have a friction angle of 41° and cohesion of 80 kPa. These results were further validated by supplementary shear testing in our laboratory on natural discontinuities. The detailed SJM calibration process for the Meliadine case study is presented in Kapinga Kalala [17].

3.3 Coupled DFN–DEM

The third process of the workflow consists of combining the DFN and the calibrated DEM for intact properties (BPM) and then assigning the SJM properties to the DFN fractures. DFN–DEM samples can be created at different scales using a simple procedure. The master DFN model (50 m x 50 m x 50 m) is randomly sampled to provide a sample of specific dimensions. This DFN sample is then merged with a calibrated intact DEM–BPM sample of the same size. The fractures are then assigned calibrated DEM–SJM properties. With this process, the contacts between bonded particles located in intact rock portions are assigned micro-mechanical properties that enable the DEM to mimic the intact rock behavior within these sections; while the bonded particles located along fractures are assigned parameters that permit the DEM to replicate the behavior of fractures.

3.4 Representative elemental volume (REV)

It is common practice to establish the Representative Elemental Volume (REV) for rock mass properties [23]. REV is defined as a volume of rock for which the size of the sample tested contains a sufficient number of defects so that the ‘‘average’’ value of a rock mass property can be reasonably consistent with repeating testing. This was done for the Meliadine rock mass peak strength properties following the methodology outlined in Esmaieli et al. [5]. Square base rectangular prisms of DFN–DEM samples with different base lengths (2.5, 5.0, 7.5, 10, and 12.5 m) but with a constant length/base ratio of 2 were created. Five samples were extracted for each base length value with their long axis in the NS direction. In this way, a total of 25 samples were tested for UCS, E and m. The results obtained for UCS are presented in Fig. 3a. It can be seen that a plateau is reached at a sample size of 7.5 m (e.g., a rectangular prism of 7.5 m x 7.5 m x 15 m). The UCS of the rock mass (UCSrm) is approximately 25–30% of the intact UCS (UCSi). The same REV was observed for E and ν. It is thus reasonable to estimate the base length of REV to be 7.5 m.

To complement the result showed in Fig. 3a, a typical stress–strain curve obtained for a DFN–DEM sample is presented in Fig. 3b. The presented curve was obtained for a 5 m x 5m x 10 m sample. The sample has an UCSrm of 37.5 MPa. The linear portion of the stress–strain curve was used to evaluate the elastic modulus of the fractured rock mass at 40 GPa. The pre-peak properties of the rock mass were evaluated in a similar fashion for all generated DFN–DEM samples.

4 BASE CASE SCENARIO ALONG THREE TESTING DIRECTIONS

At the REV sample size (7.5 m x 7.5 m x 15 m), peak strength properties (UCS, E, and ν) were evaluated on 15 samples of simulated rock masses. Five samples had their long axis parallel to the NSdirection (Y) of the rock mass, which is perpendicular to the strike of the ore body, five samples had their long axis oriented in the EW (X) direction, which is parallel to the strike of the ore body, and the five remaining samples were oriented with a vertical long axis. A schematic layout of the base case scenario samples is shown in Fig. 4.

Along the NS axis, the UCS of the fractured rock mass (UCSrm) is 0.28 of the intact rock UCS (UCSi). It is 0.09 in the EW direction and 0.10 in the vertical direction. This indicates that there is

marked anisotropy in this property. For E, a ratio of 0.5 defines the E_{rm}/E_i in the NS direction, while a ratio of 0.2 was obtained along both the EW and vertical axes. The Poisson ratio of the rock mass is identical to the one obtained for intact rock in all three tested directions.

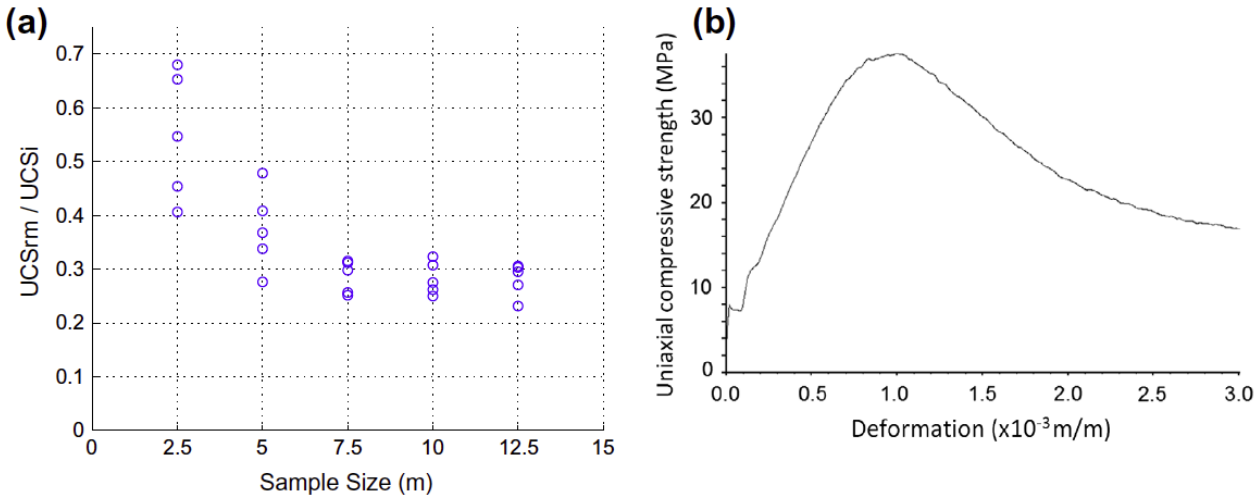

Fig. 3. (a) UCSrm/UCSi ratio results for the simulated rock mass at various sample sizes, and (b) typical stress–strain curve obtained for a DFN–DEM sample with a size of 5 m x 5 m x 10 m.

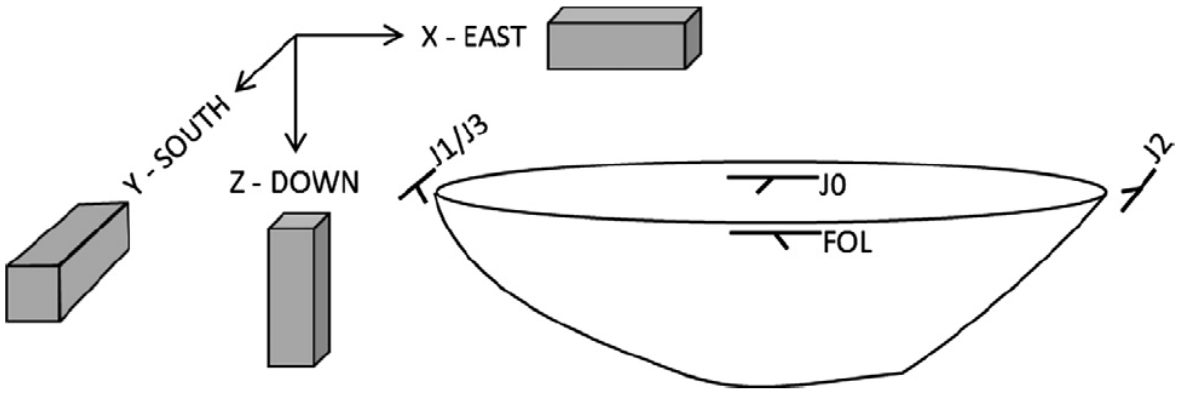

Fig. 4. Schematic layout of the samples in relation to the Meliadine gold project geometry.

5 SENSITIVITY ANALYSIS

The strengths and limitations of DEM–BPM in reproducing many features of intact rock behavior, including elasticity, fracturing, acoustic emission, damage, and post-peak softening for simulating the behavior of a rock sample have been addressed elsewhere, and Mas Ivars et al. [4] provide a good summary.

Far less work has been done on addressing the impact of varying the DFN geometric properties on the behavior of a modeled fractured rock mass. For worked examples, Bahaaddini et al. [24] and Harthong et al. [6] present numerical investigations of the effect of joint geometric properties on the mechanical properties of rock mass under uniaxial compression. In the case to which this paper pertains, it was of particular interest to identify the in situ geometric structural parameters that most affect rock mass properties at the mining site. Furthermore, since quite often some or all of the DFN model inputs are subject to sources of uncertainty, and since the DFN stochastic generation process

is also a source of variability, it was deemed important to investigate how this may affect the behavior of the DFN–DEM rock mass model.

The effect of the uncertainty or variability in the input parameters' values can be explored with a sensitivity analysis. For this, model parameters, selected by the user, are varied across a range of values and the effect on the model behavior is monitored. The scope of this study is to get a better understanding of the influence of variability and uncertainty in in situ fracture geometric properties on a DFN–DEM model's ability to quantify rock mass peak properties. Accordingly, DFN input parameter variations were kept relatively small so as to be representative of field conditions. The next section describes the sensitivity analysis performed.

5.1 Sensitivity analysis parameters

The parameters tested in the sensitivity analysis are linked to the three main components of the geometric properties of the structural regime: fracture orientation, fracture intensity and fracture size. More specifically, the parameters tested in the sensitivity analysis correspond to the input parameters of Fracture-SG [11], the code used to generate the DFNs. These are the fracture sets' mean orientation, orientation dispersion (K), volumetric intensity (P32) and area ($\bar{A}$).

5.1.1 Mean orientation of dominant fracture sets (foliation and J0)

As the dominant sets at Meliadine are the foliation and J0, the sensitivity analysis was performed varying only the aforementioned orientation parameters for those sets. The orientation properties of the J1/J3 and J2 fracture sets remained unaltered. Four alternative mean orientations were selected for the two dominant fracture sets, as shown in Fig. 5. The alternative orientations were selected on the circle located at one standard deviation from the mean value. The selected orientations correspond to the minimal and maximal dip and dip direction values along that circle. The angular standard deviation is 7° for the foliation and 11° for the J0 set. A total of eight DFNs were generated using these new inputs (4 DFNs with the modified parameters for the foliation and 4 DFNs with the modified parameters for the J0 fracture set). Fifteen samples were extracted from each DFN – 5 samples with their long axis parallel to each sampling direction. In all, 120 samples were extracted.

5.1.2 Dispersion around mean orientation values

The dispersion around the mean orientation can be evaluated using the Fisher distribution, Fisher [25]. By analogy with a normal distribution, it can be shown that the standard deviation of a Fisher distribution can be estimated from Eq. (1), [26].

$$\theta = 81°/\sqrt{K} \quad (1)$$

where θ is the ''angular standard deviation'' or ''angular dispersion'' of the Fisher distribution, and K is the Fisher constant. The θ angle was systematically varied using four ratios: 0.5, 0.75, 1.25, and 1.5. Each ratio was applied to the initial angular standard deviation associated with the four fracture sets. With these new values of dispersion, fours DFNs were generated from which 15 samples were extracted – 5 samples with their long axis parallel to each sampling direction. A total of 60 samples were extracted.

5.1.3 Fracture sets volumetric intensity (P32)

Fracture area ($\bar{A}$), and fracture intensities P31 and P32 are closely related as shown by the following equation:

$$P32 = P31 \times \bar{A} \quad (1)$$

Consequently, changing the value of one of these parameters will affect one or two of the other parameters. Three cases were thus investigated in the sensitivity analysis to identify the impact of all three parameters on DFN–DEM behavior.

The first case involved varying the ratio of total fracture area over the simulated volume. This parameter is often defined in the literature as P32, Dershowitz and Herda [27]. The P32 value was systematically varied using the same ratios as listed in Section 5.1.2. Each ratio was applied to the initial P32 values associated with the four fracture sets. Area ðAÞ was kept constant. Fours DFNs were generated, from which 15 samples were extracted, resulting in a total of 60 samples.

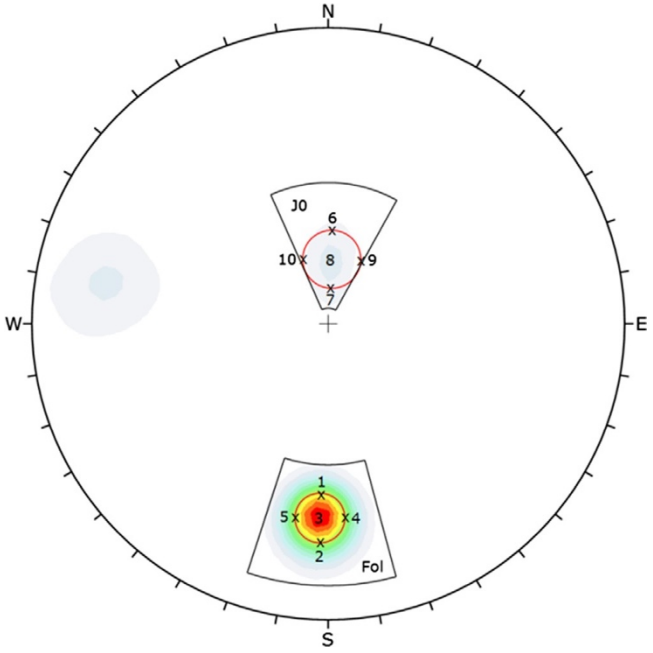

Fig. 5. Variation of mean orientations for dominant fractures sets (foliation and J0).

5.1.4 Fracture sets area ($\bar{A}$)

The second case focuses on varying set area $\bar{A}$. Intuitively, this is identical to a variation of P32 if P31 remains constant. Nonetheless, to assess the modeling results when varying $\bar{A}$, four DFNs were generated using the same ratios as listed in Section 5.1.2, but this time applied to $\bar{A}$. To keep the total number of fractures per simulated volume (P31) constant, P32 was inversely varied with $\bar{A}$. Following the same methodology, 20 samples were extracted from the DFNs; but this time, samples were only extracted with their long axis along the NS direction. Considering the required computational time and given that the results were coherent with Eq. (2), it was decided not to pursue sampling in the other directions (EW and vertical).

5.1.5 Fracture sets area ($\bar{A}$) and fractures per simulated volume (P31)

The last series of DFNs were generated varying the fracture set area ($\bar{A}$) and keeping the corresponding P32 constant, thus varying P31. This allowed assessing the importance of A and P31 as well as the sensitivity of P32 to its constituents (P31 and $\bar{A}$). The area $\bar{A}$ was varied using the four ratios (0.5, 0.75, 1.25, 1.5) applied to the initial values associated with the four fracture sets. Fours DFN were generated from which 15 samples were extracted, giving a total of 60 samples.

5.1.6 Overview of the computational effort required to perform the sensitivity analysis

The sensitivity analysis parameters were varied from a base case at REV size. This is resulting in 64 scenarios, as illustrated in Table 2 (directions DFNs). With the exception of parameter $\bar{A}$, there were 4 DFNs, sampled five times in each direction, for a total of 320 DFNs. This adds up to the 15 base case DFNs.

The 335 generated DFN samples were linked with the calibrated DEM, with the BPM properties for the intact rock and the SJM properties for the fractures. They were then tested in uniaxial compression (run parallel to their long axis – oriented with sampling directions) to evaluate their peak strength properties (UCS, E, and ν).

Table 2. Overview of the computational effort required to perform the sensitivity analysis.

	DFNs	Number of sample per direction			DFN–DEM	Scenarios
		X-EAST	Y-SOUTH	Z-DOWN		
Base case	1	5	5	5	15	3
Sensitivity analysis						
Mean orientation – Foliation	4	5	5	5	60	12
Mean orientation – J0	4	5	5	5	60	12
Dispersion of mean orientation (K)	4	5	5	5	60	12
Intensity (P32)	4	5	5	5	60	12
Area ($\bar{A}$)	4		5		20	4
Area ($\bar{A}$) + P31	4	5	5	5	60	12
Sub-total (sensitivity analysis)	24	25	30	25	320	64
Total					335	67

5.2 Statistical hypothesis testing to compare the results

The 64 scenarios resulting from the sensitivity analysis were compared with one of the three base case scenarios associated with the three sampling axis. For all scenarios, 5 samples were tested.

All 320 samples were compared for mean values and variance against a base case scenario using hypothesis testing. A t-test was done of the null hypothesis that results obtained for a given scenario and a base case scenario are independent random samples from normal distributions with equal means and equal but unknown variances, the alternative hypothesis being that the means are not equal. A 5% significance level was used to compare means. An F-test was done of the hypothesis that two independent samples (studied versus base case scenario) come from normal distributions with the same variance, the alternative being that they come from normal distributions with different variances. A 5% significance level was used to compare variances. Four types of results are possible: (1) means and variances are equal; (2) means are equal but variances are not; (3) means are not equal but variances are; and (4) means and variances are not equal.

Figs. 6–8 summarize the influence of varying DFN parameters during the sensitivity analysis on rock mass mechanical properties. Fig. 6 presents the UCS results for all scenarios; while Figs. 7 and 8 give the results for E and ν.

6 RESULTS

This section presents the results of the sensitivity analysis and its corresponding hypothesis tests. The results are given for the UCS, E, and ν of the DFN–DEM models. Figs. 6–8 are designed in a similar manner. The first column shows the results of the samples tested in the EW direction (X), the second shows the results for the NS direction (Y) and the third gives the results obtained from samples with a vertical long axis. The first row shows the results obtained while varying the mean orientation of the foliation and fracture set J0. The second row shows the outcomes of varying fracture sets area and intensity (P32). The last row shows the results obtained when varying the angular standard deviation around the fracture sets mean orientation. In every graph, the results

displayed in the center of the graphs correspond to the 5 base case samples that were tested along the sampling directions (displayed with black squares). The outcomes of the statistical hypothesis tests are illustrated using the following color coding: (1) BLUE when means and variances are equal; (2) GREEN when means are equal but variances are not; (3) MAGENTA when means are not equal but variances are; and (4) RED when means and variances are not equal. Finally, the vertical axis of the graphs shows the ratio between rock mass properties and intact rock properties while the variations imposed on the sensitivity analysis parameters are indicated on the horizontal axis.

6.1 UCS results analysis

The first row of Fig. 6 presents the results of the sensitivity analysis when varying mean fracture orientation for the foliation and J0. The results indicate that when the major axis of the samples is in the EW direction, all tested scenarios give UCSrm results similar to the base case. Since the dip direction of both foliation and J0 are perpendicular to the loading direction, it is understandable that a variation in dip does not affect UCSrm results. Samples with their long axis oriented NS are only affected by a variation in the dip of the foliation. Reducing the dip lowers the mean UCSrm of the rock mass, while increasing the dip increases the UCSrm values. This is attributable to the fact that lowering the dip of foliation facilitates shear fracturing along that fracture set, while increasing the dip angle will result in foliation being more perpendicular (74°) to the applied load during UCS testing. For the vertical samples, a variation of foliation dip also affects both the mean UCSrm results and its variances. This time, reducing the dip will increase UCSrm values, while increasing the dip will lower UCSrm results. Reducing the dip will increase the perpendicularity of the loading axis with the foliation, while increasing the dip produces foliation at 300 from the loading direction, thus facilitating shear failure. Along that testing axis, it is also possible to observe that an increase in the dip of J0 results in lower UCSrm. Increasing dip value in that direction will be favorable to shear fracturing of that set. A variation in dip direction has no significant impact on UCSrm results for that case study. This can arguably be explained by the fact that the loading axes are either almost parallel or perpendicular to the dip direction of both investigated sets, and that the variations in mean orientations used in the sensitivity analysis thus only marginally affect the results.

The second row of Fig. 6 displays the results of the sensitivity analysis when varying P32 of all fractures sets while maintaining fracture area constant. For all loading directions, reducing P32 produces a statistically significant increase in the UCSrm results. This suggests that more intact rock bridges will need to be broken to bring the rock mass specimen to failure. Increasing P32 will also result in different UCSrm in both EW and vertical loading directions but not in the NS direction. Except in one scenario, the variances were not significantly affected – during that series of analysis.

As stated before, a variation in fracture sets area should affect UCSrm in the same fashion as varying P32. To validate that with modeling results, 20 samples with a NS long axis were tested. The results can be seen in the center graph of the second row of Fig. 6. The results indicate that a variation of $\bar{A}$ or P32 will affect the UCS of the rock mass in the same way.

The last row in Fig. 6 displays the sensitivity analysis results for two parameters on UCSrm. Firstly, the impacts of varying fracture orientation dispersion around the mean values by modifying the angular standard deviation, and secondly, the impact of varying P31 and A simultaneously while keeping P32 constant are investigated.

Varying P31 and $\bar{A}$ simultaneously results in marginal impacts on the mean UCSrm. It has some impact on the variance of the UCSrm when samples were selected along the vertical axis. This suggests that any combinations of area and P31 within the studied range will not affect UCSrm if P32 remains constant. This is an interesting finding as it suggests that for the ranges of variations applied to the studied parameters, a unique P32 value consisting of a larger number of smaller fractures or of a lesser number of larger fractures will produce similar peak properties for UCSrm. The impact of varying the orientation dispersion has a minor impact on mean UCSrm and its corresponding variance.

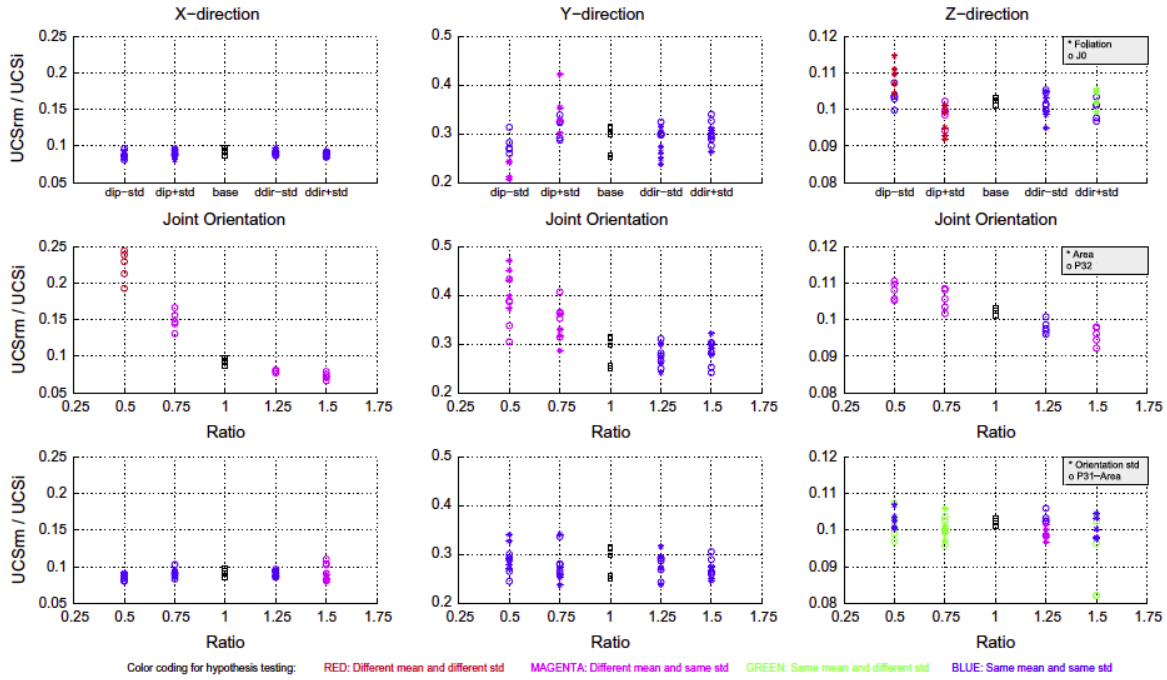

Fig. 6. Rock mass uniaxial compressive strength to intact rock uniaxial compressive strength ratio (UCSrm/UCSi) results for the sensitivity analysis along NS, EW and vertical testing directions.

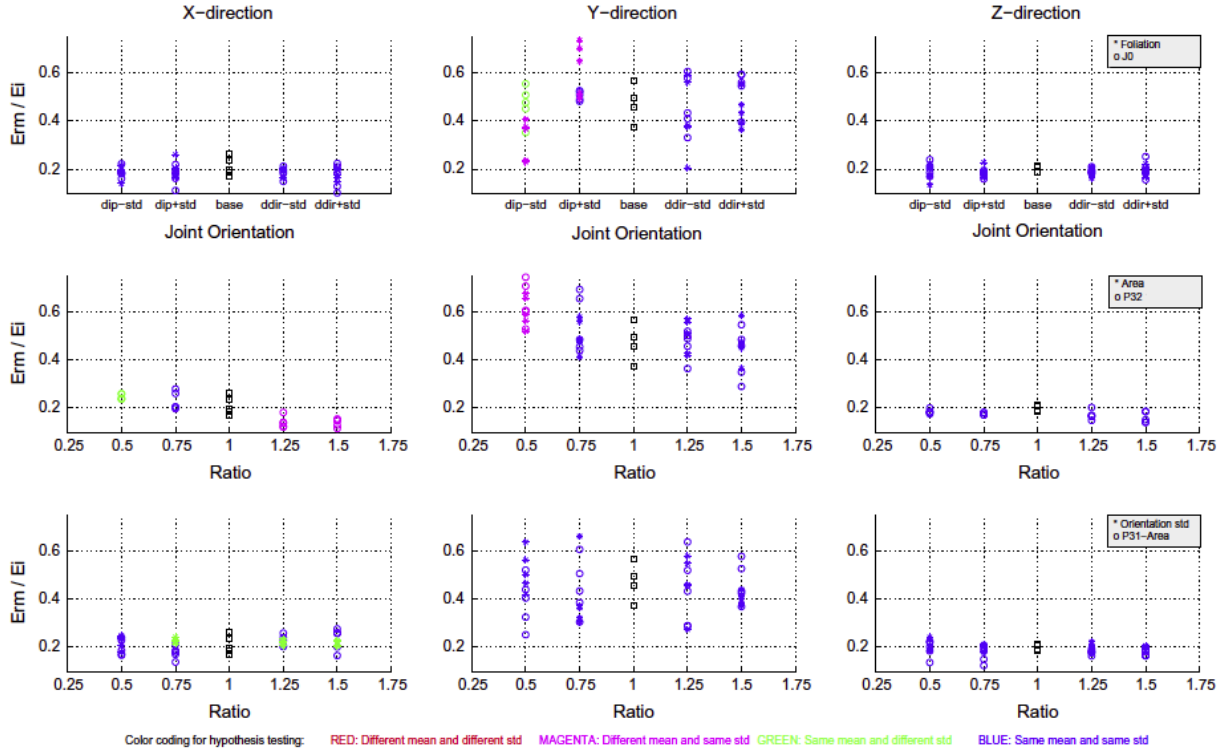

Fig. 7. Rock mass Young modulus to intact rock modulus ratios (E_{rm}/E_i) for the sensitivity analysis for NS, EW and vertical testing directions.

6.2 E results analysis

Fig. 7 displays the results of the sensitivity analysis on the rock mass Young modulus (E_{rm}). Five scenarios, where the mean E_{rm} was significantly affected by a change in the input values, were identified. For the NS direction, a variation in the dip of the foliation did result in a variation in mean Young modulus. Foliation being the dominant set in the rock mass, it can arguably be shown that increasing the dip angle of the foliation will put the foliation close to perpendicular with the loading axis thus creating a much stiffer rock mass. On the contrary, lowering the dip angle will produce a less stiff rock mass since the foliation will be at 30° from the loading axis. When the loading axis is EW, both the foliation and J0 have a dip direction perpendicular to the loading direction. Regarding the intensity, it is reasonable to assume that for that specific case study, an increase in P32 will result in a lower E_{rm}, since increasing P32 implies reducing the amount of intact rock bridges. It is also observed that a variation in P32 (ratio of 0.5) also affects the E_{rm} value in the NS direction. However a variation of P32 does not show any influence on E_{rm} in the vertical direction. As foliation is the more dominant fracture set, and has a dip of 67° in addition to being the more persistent structure, it is plausible to conclude that for samples with a vertical long axis varying P32 does not affect the E_{rm} – as it has already a maximal impact. Thus, the latter conclusions about P32 and E_{rm} tend to demonstrate that P32 variations will modify the anisotropy observed for the base case for the rock mass Young modulus. Furthermore, in some scenarios, the variances differ from the base case. In general, E_{rm} is less affected than UCSrm for the parameters studied in the sensitivity analysis.

6.3 ν Results analysis

Fig. 8 displays the sensitivity analysis results for the Poisson modulus (ν). It can be seen that varying the input parameters did not have an impact on the mean values for m. It only had a marginal impact, in three scenarios, on the variance of the results.

7 DISCUSSION

7.1 Understanding the behavior of a rock mass at Meliadine

This sensitivity analysis provided a systematically efficient way of analyzing the peak properties of a fracture rock mass at a mining project. It allowed investigating the rock mass behavior, when small but likely variations for this case scenario were applied to the geometric properties of a rock mass. It enabled identifying the most critical parameters in controlling peak rock mass properties.

It was shown that P32 was the single most important factor affecting rock mass UCS and E. Under EW and NS loading, P32 variations could change the UCSrm by up to 100%. This can be undoubtedly very significant at the design stage of a mining project. In the vertical loading direction, the variations in mean UCSrm, although statistically significant, are not critical from a design perspective.

To a lesser degree, fracture orientation can also significantly affect rock mass UCS. In the case study presented, it was shown that the dip affected the results. Dip direction could have given a similar result, but this was not the case here simply because of the specific dip direction of the foliation and J0 with respect to the NS and vertical axis. From a practical view point the results obtained in the NS direction for UCS are the only ones that could affect the design. The Young modulus can also be affected. It was shown that P32 variations under EW and NS loading could change the E_{rm} by up to 25%. Also, it was shown that the foliation dip has a significant impact on the E_{rm} in the NS direction. Therefore, from a practical design perspective, the foliation orientation and P32 in the NS direction could be the most dominant factors controlling E_{rm}. The Poisson ratio was not affected by variation in the DFN properties.

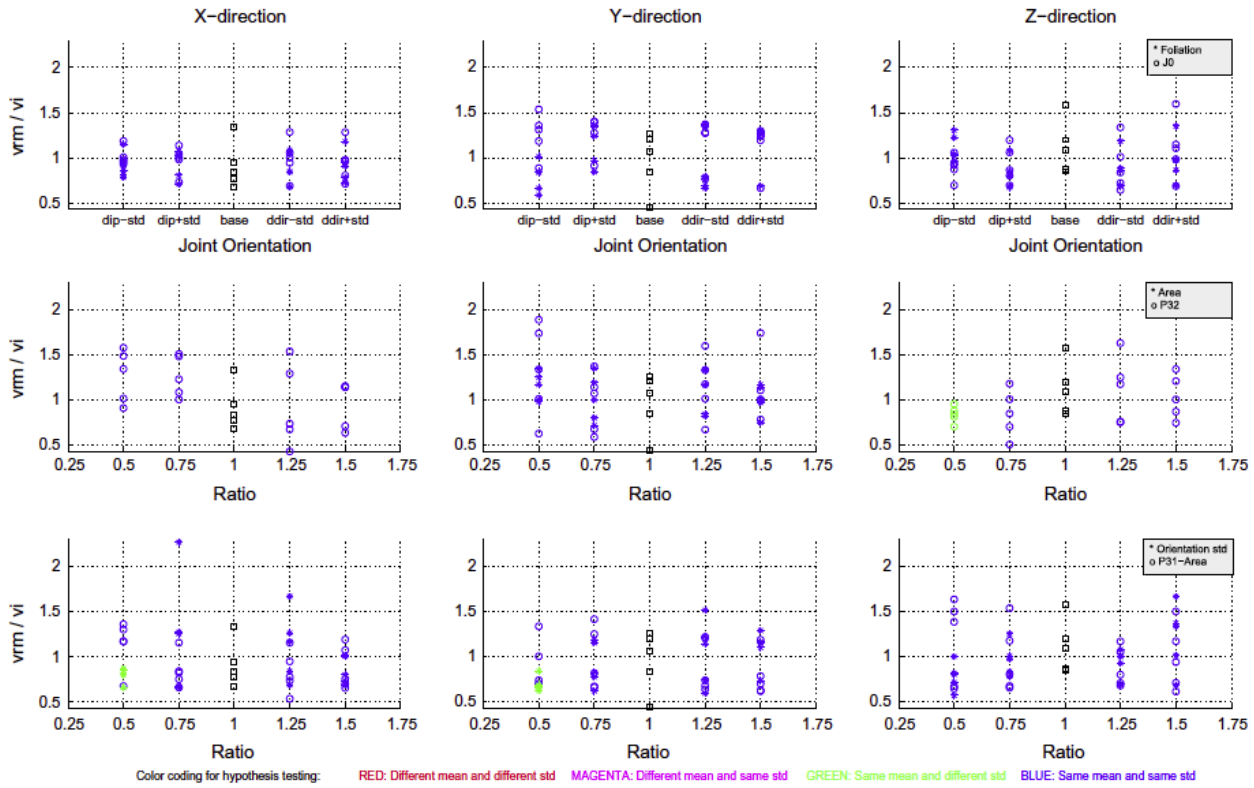

Fig. 8. Rock mass Poisson ratio to intact rock Poisson ratio (ν_{rm}/ν_i) for the sensitivity analysis for NS, EW and vertical sampling directions.

7.2 Perspective

Currently, the DFN–DEM approach cannot be routinely used to analyze rock mass mechanical properties at the engineering project scale because of computing time limitations, but it nonetheless provides a worthwhile means of characterizing the behavior of a fracture rock mass. It does complement the current approaches relying on empirical rock mass classifications to define rock mass properties at the scale of an engineering work. Furthermore, it provides a unique means of quantifying anisotropy in the rock mass properties. Finally, it offers a means of quantifying, for a given rock mass, the most critical properties in defining rock mass behavior, and it allows for defining a possible range of values for rock mass properties at the engineering project scale.

Since the common practice in rock engineering applications is to use numerical tools to assess the behavior of a rock mass surrounding an engineering work and since these numerical tools require constitutive models to describe the behavior of a rock mass, the measured values for peak rock mass properties and anisotropy obtained through DFN–DEM modeling could provide quality input values for such deterministic and probabilistic numerical analysis.

The actual approach when using DFN–DEM modeling relies, however, on a very limited number of numerical samples due to time constraints. The inherent variability in stochastic and field data is thus not well accounted for. Based on the results obtained in the sensitivity analysis, this can be critical for design purposes. Field validations will need to be conducted using back analysis at the engineering project scale in order to gain full confidence in the DFN–DEM approach.

8 CONCLUSIONS

A coupled DFN–DEM approach was used to evaluate the peak rock mass mechanical properties at REV for a case study. In addition, a sensitivity analysis was performed in order to determine the influence of varying the DFN model input parameters' values on the rock mass mechanical properties. The rock mass properties–uniaxial compressive strength, Young modulus and Poisson ratio–obtained from the sensitivity analysis were compared to the initial mechanical properties through statistical hypothesis testing. All results were reported in relation to the properties found at REV for a base case. The sensitivity analysis was performed using small variations for input parameter values similar to the ones observed in the field. For the rock mass of the case study presented, the most critical parameters affecting the peak behavior of the rock mass were found to be the intensity (P32) and the mean fracture set orientation. The analysis also provided a unique way of investigating the anisotropy of the rock mass properties. This paper provides a promising systematic quantitative approach for better identifying critical structural parameters controlling rock mass peak properties at the engineering scale. This methodology is not site specific and it can be applied at any engineering work performed in fractured rock masses.

ACKNOWLEDGEMENTS

The authors would like to acknowledge the financial support of NSERC and AEM. The authors would also like to thank AEM, Technical Service Division, for providing easy site and data access.

REFERENCES

[1] Hoek E, editor. Practical rock engineering. Rocscience; 2007.
[2] Cai M, Kaiser PK, Tasaka Y, Minami M. Determination of residual strength parameters of jointed rock masses using the GSI system. Int J Rock Mech Min Sci 2007;44(2):247–65.
[3] Alejano LR, Alonso E, Rodríguez-Dono A, Fernández-Manín G. Application of the convergence-confinement method to tunnels in rock masses exhibiting Hoek–Brown strain-softening behaviour. Int J Rock Mech Min Sci 2010;47(1):150–60.
[4] Mas Ivars D, Pierce ME, Darcel C, Reyes-Montes J, Potyondy DO, Paul Young R, et al. The synthetic rock mass approach for jointed rock mass modelling. Int J Rock Mech Min Sci 2011;48(2):219–44.
[5] Esmaieli K, Hadjigeorgiou J, Grenon M. Estimating geometrical and mechanical REV based on synthetic rock mass models at Brunswick Mine. Int J Rock Mech Min Sci 2010;47(6):915–26.
[6] Harthong B, Scholtes L, Donze F-V. Strength characterization of rock masses, using a coupled DEM–DFN model. Geophys J Int 2012;191(2):467–80.
[7] Priest SD, editor. Discontinuity analysis for rock engineering. Chapman & Hall; 1993.
[8] Read J, Stacey P. Guidelines for open pit slope design. In: Read J, Stacey P, editors. Leiden. Netherlands: CSIRO Publishing; 2009. p. 514.
[9] Meliadine Project – Camp Area Geology Map. Agnico Eagle; 2013.
[10] Dershowitz WS, Einstein HH. Characterizing rock joint geometry with joint system models. Rock Mech Rock Eng 1988;21(1):21–51.
[11] Grenon M. Fracture-SG. 2.17 ed2008. p. A fracture system generator software package.
[12] Grenon M, Hadjigeorgiou J. Applications of fracture system models (FSM) in mining and civil rock engineering design. Int J Min Reclam Environ 2012;26(1):55–73.
[13] Meyer T. Geologic stochastic modeling of rock fracture systems related to crustal faults [S.M.]: Massachusetts Institute of Technology; 1999.
[14] Dershowitz WS, editor. Rock joint systems. [Ph.D.]. Cambridge, MA: Massachusetts Institute of Technology; 1984.

[15] Grenon M, Hadjigeorgiou J. A design methodology for rock slopes susceptible to wedge failure using fracture system modelling. Eng Geol 2008;96(1– 2):78–93.
[16] Dershowitz WS. Interpretation and synthesis of discrete fracture orientation, size, shape, spatial structure, and hydrologic data by forward modeling in fractured and jointed rock masses. In: Myer LR, Godman RE, Tsang CF, editors. Conference on fractured and jointed rock masses. Lake Tahoe, California, USA:
A.A. Balkema; 1995. p. 579–86.
[17] Kapinga Kalala I. Caractérisations structurale et mécanique du massif rocheux de la fosse tiriganiaq du projet Meliadine à l'aide de la modélisation synthétique du massif rocheux [Mémoire de maitrise]. Québec: Université Laval; 2013.
[18] Potyondy DO, Cundall PA. Modeling notch-formation mechanisms in the URL Mine-by Test Tunnel using bonded assemblies of circular particles. Int J Rock Mech Min Sci 1998;35(4–5):510–1.
[19] Yoshinaka R, Osada M, Park H, Sasaki T, Sasaki K. Practical determination of mechanical design parameters of intact rock considering scale effect. Eng Geol 2008;96(3–4):173–86.
[20] Cai M, Kaiser PK, Uno H, Tasaka Y, Minami M. Estimation of rock mass deformation modulus and strength of jointed hard rock masses using the GSI system. Int J Rock Mech Min Sci 2004;41(1):3–19.
[21] Mas Ivars D, Potyondy DO, Pierce M, Cundall PA. The smooth-joint contact model. In: Schrefler BA, Perego U, editors. 8th World congress on computational mechanics/5th European congress on computational methanics and applied science and engineering. Venice: CIMME; 2008. p. a2735.
[22] Report on feasibility level pit slope design criteria for the Tiriganiaq deposit Meliadine gold project.: Golder Associates Inc.; 2010.
[23] Hudson JA, Harrison JP. Engineering rock mechanics – an introduction to the principles. Amsterdam: Elsevier Science & Technology; 2000.
[24] Bahaaddini M, Sharrock G, Hebblewhite BK. Numerical direct shear tests to model the shear behaviour of rock joints. Comput Geotechn 2013;51:101–15.
[25] Fisher RA. Dispersion on a sphere. In: Proceedings of the royal, society, vol. A217; 1953. p. 295–305.
[26] Butler RF. Statistics of paleomagnetism data. In: Scientific B, editor. Paleomagnetism: magnetic domains to geologic terranes. Boston: Oxford; 1992. p. 103–20.
[27] Dershowitz W, Herda HH. Interpretation of fracture spacing and intensity. In: Proceedings of the 1992 MRS fall meeting: symposium U, solid state ionics, June 3, 1992 – June 5, 1992. Santa Fe, NM, USA: Publ by A.A. Balkema; 1991. p. 757.